Available online at www.sciencedirect.com
ScienceDirect
Journal of Sound and Vibration 303 (2007) 46–57
JOURNAL OF SOUND AND VIBRATION
www.elsevier.com/locate/jsvi

A finite element model of vehicle–bridge interaction considering braking and acceleration

Shen-Haw Ju*, Hung-Ta Lin

Department of Civil Engineering, National Cheng-Kung University, Ta-Hsueh Road, Tainan 70101, Taiwan

Received 14 July 2005; received in revised form 1 November 2006; accepted 13 November 2006
Available online 6 March 2007

Abstract

This paper develops a finite element scheme to analyze vehicle–bridge dynamic responses due to vehicle braking and acceleration. In this model, an assumption is that the averaged vehicle acceleration at current time is known; so absolute vehicle displacements can be changed to relative vehicle displacements. Thus, the inertia force at the center of each vehicle mass can be generated. This scheme produces a linear and small displacement analysis. In the meantime, the semi-theoretical solution of a two-axle vehicle moving on a bridge was generated with the acceleration effect. Then, this scheme was used to validate the proposed finite element model with almost identical agreement. The most attraction of this model is that the theory and formulation are simple and can be added to standard dynamic finite element codes without difficulty.

1. Introduction

Investigating bridge dynamic behaviors induced by moving vehicles has passed through more than 100 years. At present, researchers can perform complicated and actual vehicle–bridge analyses. The literature is extensive for the bridge dynamic response due to moving vehicles with constant speed. However, not much investigation was oriented toward the dynamic response of bridges passed by moving vehicles with non-uniform speed (braking or acceleration). In early studies, Fryba [1,2] researched the foundation characteristics of a beam due to a rolling mass under braking effect, and also studied the quasi-static distribution of braking and starting forces in rails and bridge. Afterward, investigation on the dynamic response of highway bridges under vehicle braking was reported by Kishan and Traill-Nash [3]. They indicated that vehicle braking may contribute significantly to bridge response, and that the resulting impact factors may exceed those adopted in current design practice. Gupta and Traill-Nash [4] investigated a dynamic behavior of single span bridge due to vehicular load with road surface irregularities and braking of vehicle. Mulcahy [5] presented a method for the calculation of dynamic response of single span bridges due to a three-axle tractor–trailer vehicle. The method takes account of vehicle acceleration or braking and road roughness. Krylov [6] investigated the ground vibration due to the vehicle with a constant acceleration from rest to a constant speed. Toth and Ruge [7] analyzed the longitudinal behavior of long railway bridges due to moving train braking. Yang and Wu [8]

*Corresponding author. Tel.: +886 6 2757575 63119; fax: +886 6 2358542.
E-mail address: juju@mail.ncku.edu.tw (S.-H. Ju).

0022-460X/$ - see front matter © 2007 Published by Elsevier Ltd.
doi:10.1016/j.jsv.2006.11.034

developed suitable numerical models for handing both the vehicle and bridge responses; moreover, they investigated the behavior of a bridge caused by a vehicle in deceleration. Berghuvud [9] performed the modeling and simulation of the strongly nonlinear dynamic interaction between vehicle and track in braked conditions. Hu and Han [10] presented a nonlinear dynamic model of 9 degrees of freedom for four-wheel-steering vehicles. This model includes the pitch and roll of the vehicle body, the motion of 4 wheels in the accelerating or braking process. Guner et al. [11] developed a dynamic model for dynamic and thermal analysis of the braking phenomenon. Using this model, the equation of motion of a car has been derived for straight line braking. Law and Zhu [12] studied the dynamic responses of a multi-span continuous bridge under a moving vehicle by considering the effect of interaction between the road surface roughness and the braking of vehicle.

This study developed a simple finite element model to simulate vehicle–bridge dynamic problems for the braking and acceleration of moving vehicles. In the meantime, we proposed the semi-theoretical solution to validate this finite element method. As we know, this type of validation is limited in the literature. The most attraction of this model is that the theory and formulation are simple and can be added to dynamic finite element codes without difficulty. Moreover, very complicated vehicles can be appropriately modeled using this proposed method with the same approach of a standard finite element method.

2. Equations of a moving two-axle system

The main purpose of this section is to evaluate a semi-theoretical solution to validate the finite element method mentioned in Section 4. Fryba [13] generated the formulations of a two-axle vehicle moving on a simply supported beam loaded in the gravity direction (z direction). This study added the horizontal (x direction) spring and damper into Fryba's solution so that the braking and acceleration could be included. In this paper, the x direction is the bridge longitudinal direction and the z direction is the gravity direction. Since, we solved the current equations using numerical methods, the bridge is not necessary to be simply supported. Fig. 1 shows a two-axle vehicle with 7 degrees of freedom including rigid mass rotation (ϕ), rigid mass, wheel 1 and wheel 2 displacements (v_3, v_1 and v_2) in the z direction and those (u_3, u_1 and u_2) in the x direction. The bridge surface where vehicles move is assumed in the x direction with a length of L. In the intervals $0 \leqslant x \leqslant L$, the moment equilibrium at the rigid body center is

$$-I\ddot{\phi} - D_1(Z_1 + Z_{b1}) + D_2(Z_2 + Z_{b2}) - (F_1 + F_2)H_c = 0, \tag{1}$$

where

$$Z_1 = k_1(v_3 - D_1\phi - v_1), \tag{2}$$

$$Z_2 = k_2(v_3 - D_2\phi - v_2), \tag{3}$$

$$Z_{b1} = c_1(\dot{v}_3 - D_1\dot{\phi} - \dot{v}_1), \tag{4}$$

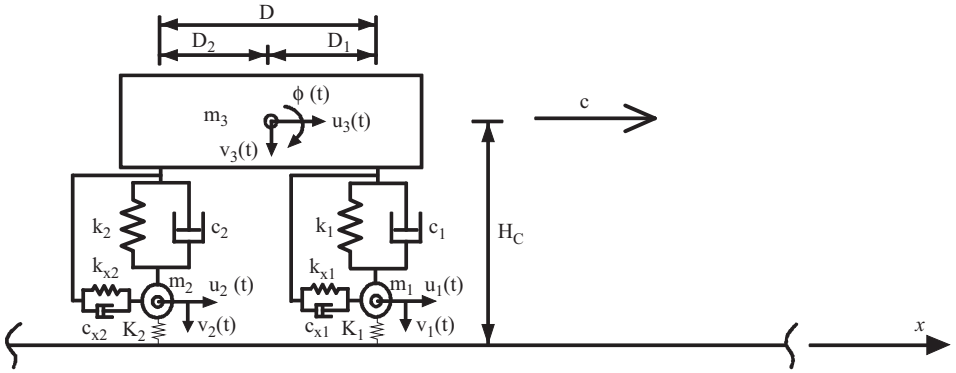

Fig. 1. Two-axle vehicle model with vertical and horizontal spring–dampers.

$$Z_{b2} = c_2(\dot{v}_3 - D_2\dot{\phi} - \dot{v}_2), \tag{5}$$

$$-F_1 = (u_3 - \phi H_c - u_1)k_{x1} + (\dot{u}_3 - \dot{\phi}H_c - \dot{u}_1)c_{x1}, \tag{6}$$

$$-F_2 = (u_3 - \phi H_c - u_2)k_{x2} + (\dot{u}_3 - \dot{\phi}H_c - \dot{u}_2)c_{x2}, \tag{7}$$

where I is the mass of inertia of the rigid body, c_1, c_2, c_{x1} and c_{x2} are the dampers, k_1, k_2, k_{x1} and k_{x2} are the springs and H_c, D_1 and D_2 are the distances as shown in Fig. 1.

The equations of horizontal and vertical equilibriums at the rigid body center are

$$-m_3\ddot{u}_3 + F_1 + F_2 = 0, \tag{8}$$

$$-m_3\ddot{v}_3 - (Z_1 + Z_{b1}) - (Z_2 + Z_{b2}) = 0, \tag{9}$$

where m_3 is the mass of the rigid body.

The equations of horizontal and vertical equilibriums at wheel i ($i = 1, 2$) are

$$-m_i\ddot{u}_i + F_i + R_{ix} = 0, \tag{10}$$

$$P_i + P_{3i} - m_i\ddot{v}_i + Z_i + Z_{bi} - R_i = 0, \tag{11}$$

$$R_{ix} = K_{ix}[u_i - \varepsilon_i u(x_i, t)], \tag{12}$$

$$R_i = K_i[v_i - \varepsilon_i v(x_i, t) - r_i(x_i)], \tag{13}$$

where m_i is the mass of wheel i, P_i ($= m_i g$, g = gravity) is the weight of wheel i and P_{3i} ($= m_3 g(D - D_i)/D$) is the load at wheel i from the weight of the rigid body, R_{ix} and R_i are x and z moving forces by which the wheel i acts on beam at point x_i, K_{ix} and K_i are the spring constants in x and z directions to simulate the elastic layer of the beam surface, $u(x_i, t)$ and $v(x_i, t)$ are the x and z displacement of the beam at x_i, ε_i is zero for wheel i outside the beam domain and is one for wheel i inside the beam domain and $r_i(x_i)$ is the road irregularity at x_i in the z direction.

The above equations can be re-arranged to be a matrix form as follows:

$$[M]\begin{Bmatrix} \ddot{\phi} \\ \ddot{v}_3 \\ \ddot{v}_1 \\ \ddot{v}_2 \\ \ddot{u}_3 \\ \ddot{u}_1 \\ \ddot{u}_2 \end{Bmatrix} + [C]\begin{Bmatrix} \dot{\phi} \\ \dot{v}_3 \\ \dot{v}_1 \\ \dot{v}_2 \\ \dot{u}_3 \\ \dot{u}_1 \\ \dot{u}_2 \end{Bmatrix} + [K]\begin{Bmatrix} \phi \\ v_3 \\ v_1 \\ v_2 \\ u_3 \\ u_1 \\ u_2 \end{Bmatrix} = \{P_F\}, \tag{14}$$

where

$$[M] = \begin{bmatrix} I & 0 & 0 & 0 & 0 & 0 & 0 \\ 0 & m_3 & 0 & 0 & 0 & 0 & 0 \\ 0 & 0 & m_1 & 0 & 0 & 0 & 0 \\ 0 & 0 & 0 & m_2 & 0 & 0 & 0 \\ 0 & 0 & 0 & 0 & m_3 & 0 & 0 \\ 0 & 0 & 0 & 0 & 0 & m_1 & 0 \\ 0 & 0 & 0 & 0 & 0 & 0 & m_2 \end{bmatrix},$$

$$[C]=\begin{bmatrix} D_1^2c_1+D_2^2c_2+H_c^2(c_{x1}+c_{x2}) & D_1c_1-D_2c_2 & -D_1c_1 & D_2c_2 & -H_c(c_{x1}+c_{x2}) & H_cc_{x1} & H_cc_{x2} \\ D_1c_1-D_2c_2 & c_1+c_2 & -c_1 & -c_2 & 0 & 0 & 0 \\ -D_1c_1 & -c_1 & c_1 & 0 & 0 & 0 & 0 \\ D_2c_2 & -c_2 & 0 & c_2 & 0 & 0 & 0 \\ -H_c(c_{x1}+c_{x2}) & 0 & 0 & 0 & c_{x1}+c_{x2} & -c_{x1} & -c_{x2} \\ H_cc_{x1} & 0 & 0 & 0 & -c_{x1} & c_{x1} & 0 \\ H_cc_{x2} & 0 & 0 & 0 & -c_{x2} & 0 & c_{x2} \end{bmatrix},$$

$$[K]=\begin{bmatrix} D_1^2k_1+D_2^2k_2+H_c^2(k_{x1}+k_{x2}) & D_1k_1-D_2k_2 & -D_1k_1 & D_2k_2 & -H_c(k_{x1}+k_{x2}) & H_ck_{x1} & H_ck_{x2} \\ D_1k_1-D_2k_2 & k_1+k_2 & -k_1 & -k_2 & 0 & 0 & 0 \\ -D_1k_1 & -k_1 & k_1 & 0 & 0 & 0 & 0 \\ D_2k_2 & -k_2 & 0 & k_2 & 0 & 0 & 0 \\ -H_c(k_{x1}+k_{x2}) & 0 & 0 & 0 & k_{x1}+k_{x2} & -k_{x1} & -k_{x2} \\ H_ck_{x1} & 0 & 0 & 0 & -k_{x1} & k_{x1} & 0 \\ H_ck_{x2} & 0 & 0 & 0 & -k_{x2} & 0 & k_{x2} \end{bmatrix}$$

$$\{P_F\}=\begin{Bmatrix} 0 \\ 0 \\ P_1+P_{31}-R_1 \\ P_2+P_{32}-R_2 \\ 0 \\ -R_{1x} \\ -R_{2x} \end{Bmatrix}.$$

Eq. (14) can be used to calculate the dynamic response of the two-axle vehicle, in which only the displacements ($u(x_i, t)$ and $v(x_i, t)$) at wheels 1 and 2 of the force terms R_1, R_2, R_{1x} and R_{2x} are required from the bridge. For the bridge structure, these forces are applied to the current locations of wheels 1 and 2 in x and z directions. If these forces are known, the bridge structural analysis is a linear dynamic problem, which can be accurately solved using a traditional Newmark finite element method. Since these forces and displacements u_1, u_2, v_1 and v_2 are coupled together, we used following procedures to solve this bridge–vehicle problem.

(1) Find R_1, R_2, R_{1x} and R_{2x} using the displacements of the last time step.
(2) Solve Eq. (14) at the current time step using the Newmark method.
(3) Solve the bridge dynamic analysis using the Newmark finite element method.
(4) If Eps≦0.0001, the solution is convergent, and go to Step (1) for the next time step.

$$\text{Eps}=\frac{|{}_nR_1-{}_{n-1}R_1|+|{}_nR_2-{}_{n-1}R_2|+|{}_nR_{1x}-{}_{n-1}R_{1x}|+|{}_nR_{2x}-{}_{n-1}R_{2x}|}{|{}_nR_1|+|{}_nR_2|+|{}_nR_{1x}|+|{}_nR_{2x}|} \tag{15}$$

where Eps is the convergence tolerance and 0.0001 is set in this study, n means the current iteration and $n-1$ means the last iteration.

(5) If Eps > 0.0001, find R_1, R_2, R_{1x} and R_{2x} using the displacements of this iteration, and go to Step (2).

In the Newmark analysis, a very small time step length of 1E–6s was used to improve the numerical convergence. The above scheme coupled with Fryba's theoretical vehicle solution and the bridge finite element solution, which are different from the traditional finite element solution of Section 4. Thus, this method will be used to validate the accuracy of the proposed finite element method. It is noted that this semi-theoretical

method is only suitable to a two-axle vehicle moving on two-dimensional bridges. However, the proposed finite element method of Section 4 can be deal with a series of complicated vehicles moving on three-dimensional bridges.

3. Assumptions and equations of braking and acceleration

For the braking or acceleration of a vehicle, there are extra-applied forces in the system, such as friction forces between road and wheels and acceleration or deceleration forces generated by the engine. Generally, it is difficult to locate the position of those applied force precisely. In this study, we assume that the averaged vehicle acceleration (a_0) at current time is known, which is reasonable since people usually control the vehicle by setting an appropriate acceleration or deceleration. Thus, the inertia force of each mass in the vehicle can be generated. At each mass location, the position, velocity and acceleration in the x direction are

$$u_i = \bar{u}_i + v_0 t + \iint a_0 \mathrm{d}t\,\mathrm{d}t, \tag{16}$$

$$\dot{u}_i = \dot{\bar{u}}_i + v_0 + \int a_0 \mathrm{d}t, \tag{17}$$

$$\ddot{u}_i = \ddot{\bar{u}}_i + a_0, \tag{18}$$

where u_i, $\dot{u}_i$ and $\ddot{u}_i$ ($i = 1, 3$) are absolute displacements, velocities and accelerations of masses 1, 2 and 3, $\bar{u}_i, \dot{\bar{u}}_i$ and $\ddot{\bar{u}}_i$ ($i = 1, 3$) are relative displacements, velocities and accelerations of masses 1, 2 and 3, v_0 is the initial velocity and a_0 is the current acceleration.

Substitute Eqs. (16)–(18) into Eq. (14) to obtain the following equation:

$$[M]\begin{Bmatrix} \ddot{\phi} \\ \ddot{v}_3 \\ \ddot{v}_1 \\ \ddot{v}_2 \\ \ddot{\bar{u}}_3 \\ \ddot{\bar{u}}_1 \\ \ddot{\bar{u}}_2 \end{Bmatrix} + [C]\begin{Bmatrix} \dot{\phi} \\ \dot{v}_3 \\ \dot{v}_1 \\ \dot{v}_2 \\ \dot{\bar{u}}_3 \\ \dot{\bar{u}}_1 \\ \dot{\bar{u}}_2 \end{Bmatrix} [K]\begin{Bmatrix} \phi \\ v_3 \\ v_1 \\ v_2 \\ \bar{u}_3 \\ \bar{u}_1 \\ \bar{u}_2 \end{Bmatrix} = \{\bar{P}_F\}, \tag{19}$$

where

$$\{\bar{P}_F\} = \{P_F\} + \begin{Bmatrix} 0 \\ 0 \\ 0 \\ 0 \\ -m_3 a_0 \\ -m_1 a_0 \\ -m_2 a_0 \end{Bmatrix}. \tag{20}$$

The above equation can solve the vehicle dynamic response due to the vehicle acceleration. To solve the bridge dynamic response, the contact forces at wheels 1 and 2 in the x direction need to be modified as follows:

$$\bar{R}_{1x} = R_{1x} - m_1 a_0 - m_3 a_0 \frac{D_2}{D}, \tag{21}$$

$$\bar{R}_{2x} = R_{2x} - m_2 a_0 - m_3 a_0 \frac{D_1}{D}. \tag{22}$$

Replacing R_{1x} and R_{2x} by $\bar{R}_{1x}$ and $\bar{R}_{2x}$ for the friction forces on the bridge structure, one can solve the bridge dynamic response due to the vehicle acceleration.

4. Finite element solution

Moving vehicles contain car bodies, bogies, wheel-axis sets, springs and dampers, which are modeled as the combination of moving wheel elements, spring–damper elements, lumped mass and rigid links. The vehicle is assumed to move in the X direction (road direction), the vertical direction is in the Z direction and the Y direction is perpendicular to the road. If vehicles move in other directions, a transformation should be used.

4.1. Moving wheel element

The moving wheel element contains a stiffness k_r to model the elastic layer between the road and wheel as shown in Fig. 2. The direction of this element can be in the global X, Y or Z direction. The element includes a wheel node and a number of target nodes. The current wheel position is known, so the two target nodes where the wheel node is located between them can be found. If the two target nodes and the wheel node are nodes 1,3 and 2 respectively, the stiffness of this 3-node element for the nodal displacements (X_1, θ_1, X_2, X_3, θ_3) is

$$[S] = [T]^{\mathrm{T}} \begin{bmatrix} k_r & -k_r \\ -k_r & k_r \end{bmatrix} [T] \tag{23}$$

in which X_1, θ_1, X_3 and θ_3 are the translations and rotations at target nodes 1 and 3, X_2 is the translation of the wheel node and

$$[T] = \begin{bmatrix} [T_1] \\ [T_2] \end{bmatrix}, \tag{24}$$

where $[T_1] = \begin{bmatrix} 0 & 0 & 1 & 0 & 0 \end{bmatrix}$, $[T_2] = [N_1 \quad N_2 \quad 0 \quad N_3 \quad N_4]$, $N_1 = 1 - (3X_2^2/L^2) + (2X_2^3/L^3)$, $N_2 = -X_2[1 - (2X_2/L) + (X_2^2/L^2)]$, $N_3 = (3X_2^2/L^2) - (2X_2^3/L^3)$ and $N_4 = (X_2^3/L^2) - (X_2^2/L)$. ($N_i =$ the cubic Hermitian interpolation functions).

The load F including all the trainload on the wheel is equilibrium on the system, so this load F on node 2 should be transformed into nodes 1 and 3 to obtain the force vector $\{f\}$ as follows:

$$\{f\} = [T_2]^{\mathrm{T}} F. \tag{25}$$

The above wheel element can be used with beam elements. If wheel elements contain damper or mass, the unsymmetrical stiffness matrix must be used. The reason is because the velocity field of node 2 requires the derivation of shape functions. To overcome this problem, we used the stiffness without damping and mass to model the road elastic layer. Then, the spring–damping and lumped mass elements discussed in next section can be connected to this element directly, because the responses at node 2 are explicit and the derivation of shape functions is unnecessary. To evaluate the irregularity between the road and wheel, the element forces of Eq. (25) are required to add into the global force vector $\{f_r\}$.

$$\{f_r\} = [T_2]^{\mathrm{T}} k_r r(X), \tag{26}$$

where $r(X)$ is a function of the road or rail irregularity and X is the wheel location in the moving wheel direction (X axes).

The moving wheel element contains a stiffness k_r without damping to model the elastic layer between the road and wheel, so the stiffness matrix can be symmetric. This scheme is similar to the penalty method where a

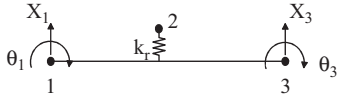

Fig. 2. Moving wheel element.

constant should be defined. Since the current method is linear elastic without iteration procedures, k_r will not cause the problem of solution instability.

4.2. Spring–damper and lumped mass elements

The spring–damper element contains stiffness k_v and damping c_v as shown in Fig. 3. The direction of this element can be in the X, Y or Z direction. The stiffness and damping matrices of this element are

$$[S] = \begin{bmatrix} s & -s \\ -s & s \end{bmatrix}. \tag{27}$$

For the damping matrix $s = c_v$ and for stiffness matrix $s = k_v$. $[S]$ is the damping or stiffness matrix that can be directly added to the global stiffness or damping matrix.

The lumped mass matrix is a diagonal matrix as follows:

$$[S] = [\backslash \quad m \quad m \quad m \quad I_x \quad I_y \quad I_z \quad \backslash], \tag{28}$$

where m is the mass, I_x, I_y and I_z are the moment of inertia in three global directions.

4.3. Rigid link effect

Rigid links connect the above finite elements with rigid bodies. For small deformation in a rigid body, if the force F_i^S is known in the global i direction ($i = X$, Y or Z) at a slave node, the force and moments at the mass center, called master node, can be calculated as follows:

$$F_i^M = F_i^S, \tag{29}$$

$$\begin{Bmatrix} M_Y^M \\ M_Z^M \end{Bmatrix} = \begin{bmatrix} -\Delta Z \\ \Delta Y \end{bmatrix} F_X^S, \quad \begin{Bmatrix} M_X^M \\ M_Z^M \end{Bmatrix} = \begin{bmatrix} \Delta Z \\ -\Delta X \end{bmatrix} F_Y^S \quad \text{and} \quad \begin{Bmatrix} M_X^M \\ M_Y^M \end{Bmatrix} = \begin{bmatrix} -\Delta Y \\ \Delta X \end{bmatrix} F_Z^S \text{ or } \{M^M\} = [D] F_i^S, \tag{30}$$

where $(\Delta X, \Delta Y, \Delta Z)$is the coordinate difference between the master and slave nodes, M_X^M, M_Y^M and M_Z^M are the moments at the master node in the global X, Y and Z direction, respectively.

For a n-degree-of-freedom mass, damping or stiffness matrix ($[S^S]$) and the force vector ($\{F^S\}$) with a slave degree of freedom (assume at kth degree of freedom), $[S^M]$ and $\{F^M\}$ at the master node are

$$[S^M] = \begin{bmatrix} & [I] & \\ [0]_1 & [D] & [0]_2 \end{bmatrix} [S^S] \begin{bmatrix} & [I] & \\ [0]_1 & [D] & [0]_2 \end{bmatrix}^{\mathrm{T}} \text{ or } [S^M] = [T][S^S][T]^T, \tag{31}$$

$$\{F^M\} = [T]\{F^S\}, \tag{32}$$

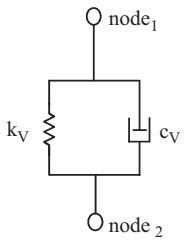

Fig. 3. Spring–damper element.

where $[I]$ is the $n \times n$ unit matrix, $[0]_1$ and $[0]_2$ are zero matrices and $[D]$ is obtained from Eq. (30). After the transformation, the kth degree of freedom of $[S^M]$ is the translation degree of freedom at the master node, and two extra-degrees of freedom $\{M^M\}$ in Eq. (30) are contained at the last two degrees of freedom of the new matrix $[S^M]$. Usually, an element contains parts of slave and parts of normal degrees of freedom. We can use Eq. (31) to do the transformation for each slave degree of freedom successfully.

4.4. Braking and acceleration

The assumptions are the same as those of Section 3, all the displacements, velocities and accelerations at vehicles in the motion (X) direction are relative to current averaged displacement, velocity and acceleration (similar in Eqs. (16)–(18)). For vehicles, the stiffness and damping forces are null for the averaged vehicle displacement and velocity, so the unknown terms change to the relative displacement and velocity. The mass forces due to the averaged vehicle acceleration in the motion direction can be calculated explicitly as inertia forces (masses multiplying averaged vehicle acceleration). Thus, all the mass locations at vehicles are subjected to inertia forces in the negative acceleration direction. After the above procedure, wheel element stiffness matrices are added to the finite element model. Since there are wheel elements connecting vehicles and bridges, the contact forces between them will be calculated automatically, so the applied forces (Eqs. (21) and (22)) subjected to bridges are not required. The above procedures produce a linear small-displacement finite element analysis for the vehicle–bridge dynamic problem. The advantage of this model is that the formulation is simple. The disadvantage is that the mass, damping and stiffness matrices vary with wheel position, which needs to be solved at each time step. This condition is not serious, since for a problem with large degrees of freedom the efficient conjugate gradient method [14] is often used to solve the matrix equation. At this time, solving a new matrix equation at each time step is necessary. This moving vehicle dynamic analysis with large degrees of freedom can be found in our previous investigations [15–17].

5. Validations

This section uses the semi-theoretical solution of Section 3 to validate the finite element method of Section 4. The vehicle as shown in Fig. 1 is a rigid body containing two spring–dampers. The parameters of this vehicle are $D = 14\,\text{m}$, $D_1 = D_2 = 7\,\text{m}$, $H_c = 2\,\text{m}$, $m_1 = m_2 = 1\text{e}3\,\text{kg}$, $m_3 = 18\text{e}3\,\text{kg}$, $I = 1\text{e}5\,\text{kg m}^2$, $c_1 = c_2 = c_{1x} = c_{2x} = 2\text{e}4\,\text{kg s}$, $k_1 = k_2 = k_{1x} = k_{2x} = 8\text{e}6\,\text{N/m}$, $K_1 = K_2 = 3.85\text{e}10\,\text{N/m}$ (K_i is the spring constant of ties). For the initial condition, the first wheel just begins to enter the bridge. The bridge material properties are Young's modulus of $2\text{e}11\,\text{N/m}^2$, mass per unit length of $4\text{e}3\,\text{kg/m}$, section area of $0.2\,\text{m}^2$, moment of inertia of $0.03\,\text{m}^4$ and damping ratio of zero. The Newmark method was used to solve the two schemes with the Newmark constants of 0.5 and 0.25. The time step length is 1e–6s for the semi-theoretical scheme of Section 3 and 1e–3s for the finite element method of Section 4.

In the finite element scheme, the vehicle is modeled by two wheel elements, two spring–damper elements and three lumped masses (wheel 1, wheel 2 and the rigid body). The master node is located at the center of the lumped mass, and the upper nodes of the two spring–damper elements are slave nodes controlled by this master node. The next two sub-sections compare the semi-theoretical and finite element solutions due to the change of the bridge structure, vehicle speed and acceleration.

5.1. One-bay bridge with two piers under rigid connections

In Fig. 4, the two-axle vehicle moves on a one-bay bridge with two piers, in which the bridge length is 40 m and the pier height is 10 m. The connections between the bridge and piers are rigid. The mesh of the bridge contains 20 equal-space elements for the semi-theoretical scheme of Section 3 and six equal-space elements for the finite element scheme of Section 4. Each pier contains four elements for both schemes. The vehicle initial velocity, final velocity and acceleration are 30, 40 and $5\,\text{m/s}^2$ for case 1 and 30, 40 and $2\,\text{m/s}^2$ for case 2. Fig. 5 shows the comparison of the displacements on beam and mass centers using the two schemes. In this

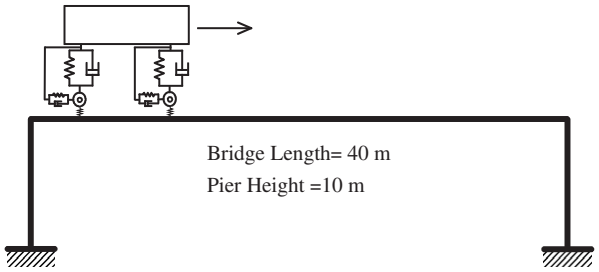

Fig. 4. The two-axle vehicle moves on a one-bay bridge with two piers.

figure, solid and dashed lines are duplicate, which indicates that the results of the two schemes are almost identical.

5.2. Three-bay continuous bridge with four piers under rigid connections

In Fig. 6, the two-axle vehicle moves on a three-bay bridge with four piers, in which the bridge bay length is 40 m and the pier height is 15 m. The connections between the bridge and piers are rigid. The mesh of the bridge contains 60 equal-space elements for the semi-theoretical scheme of Section 3 and 18 equal-space elements for the finite element scheme of Section 4. Each pier contains four elements for both schemes. The vehicle initial velocity, final velocity and acceleration are 30, 45 and 5 m/s^2 for case 1, 30, 45 and 2 m/s^2 for case 2 and 40, 30 and -5 m/s^2 for case 3. Fig. 7 shows the comparison of the displacements on beam and mass centers using the two schemes. Similar to Example 1, this figure indicates that the comparison is almost identical.

The above two examples indicate that the bridge vertical response is not so sensitive as the bridge longitudinal response due to vehicle braking or acceleration, and this condition will be more serious when the bridge contains high piers. The resonance may be invoked due to a series of vehicles, such as moving trains. Thus, It will produce considerable errors if one only considers steady-static results for vehicle braking and acceleration.

6. Conclusions

This paper developed a finite element scheme to calculate vehicle–bridge dynamic responses due to vehicle braking and acceleration. First, the semi-theoretical solution of a two-axle vehicle moving on a bridge was generated with the acceleration effect, and this scheme was used to validate the proposed finite element model. In the semi-theoretical scheme, springs and dampers in the motion direction were added into Fryba's solution so that the braking and acceleration could be included. Since the bridge was solved using the traditional finite element method, this semi-theoretical scheme can work out the two-axle–vehicle–bridge dynamic problem with various bridge shapes.

In the vehicle acceleration problem, we assume that the averaged vehicle acceleration at current time is known; so absolute vehicle displacements can be changed to relative vehicle displacements. Thus, the inertia force at the center of each vehicle mass can be generated. This scheme used into a traditional finite element method produces a linear and small displacement analysis. Numerical comparisons indicate that the results of the semi-theoretical and finite element analyses are almost identical. The most advantage of the proposed finite element model is that the theory and formulations are very simple with symmetric stiffness and damping matrices, so it can be added to a standard dynamic finite element codes easily. Moreover, very complicated vehicle models can be assembled using the proposed elements as simple as the traditional linear-elastic and small-deformation finite element method.

The numerical examples of this paper indicate that the bridge longitudinal response is more sensitive than the bridge vertical response when the vehicle braking or acceleration is active, especially for higher piers.

The resonance may be invoked due to a series of vehicles, so only using steady-static results for vehicle braking or acceleration may produce large errors. The proposed finite element method can give a simple and accurate approach to calculate the effect of vehicle braking and acceleration.

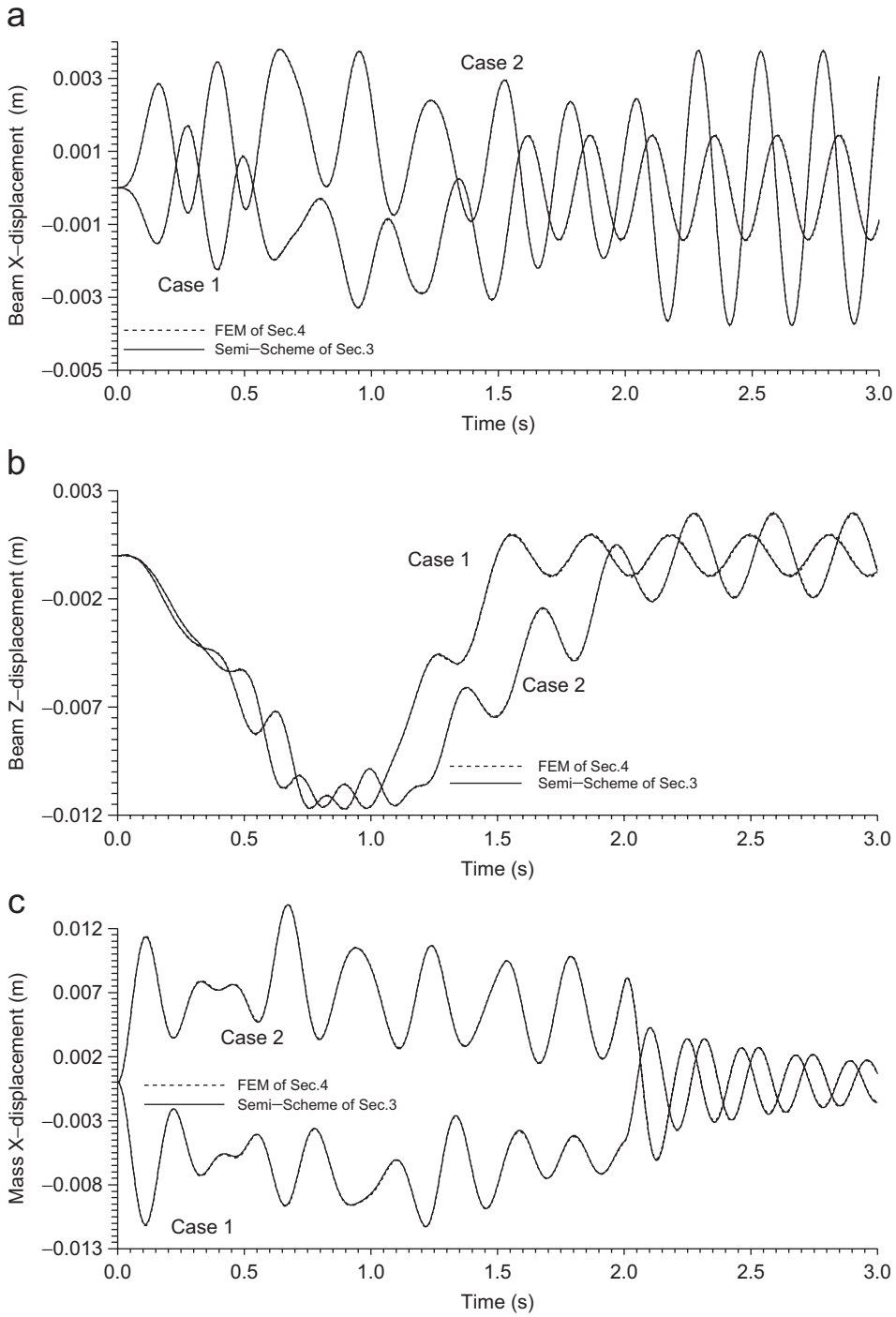

Fig. 5. Displacements at beam and mass centers for example 1. (The dashed and solid lines are overlapped, which indicates that the two solutions are almost identical.)

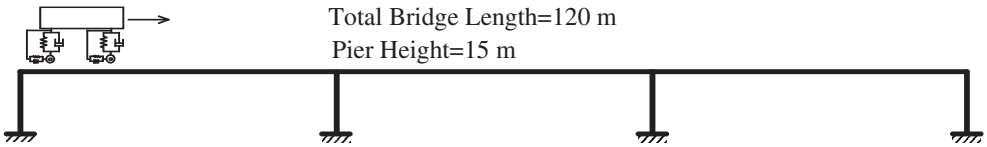

Fig. 6. The two-axle vehicle moves on a three-bay bridge with four piers.

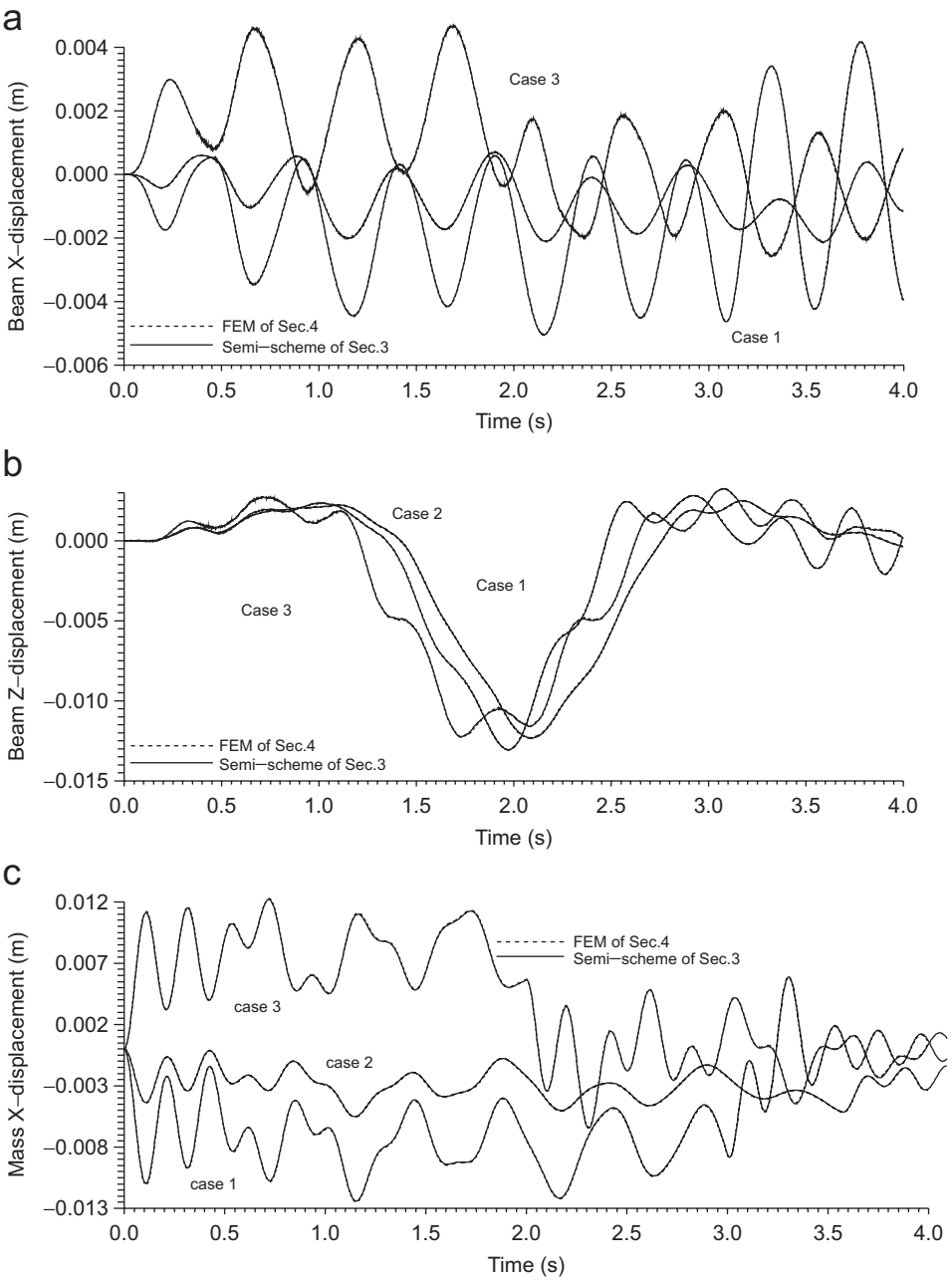

Fig. 7. Displacements at beam and mass centers for example 2. (The dashed and solid lines are overlapped, which indicates that the two solutions are almost identical.)

Acknowledgment

This study was supported by the National Science Council, Republic of China, under Contract No. NSC90-2211-E-006-063.

References

[1] L. Fryba, Response of a beam to a rolling mass in the presence of adhesion, *Acta Technica CSAV* 19 (6) (1974) 673–687.
[2] L. Fryba, Quasi-static distribution of braking and starting forces in rails and bridge, *Rail International* 5 (11) (1974) 698–716.
[3] H. Kishan, R.W. Traill-Nash, A modal method for calculation of highway bridge response with vehicle braking, *Civil Engineering Transactions, Institution of Engineers, Australia* 19 (1) (1977) 44–50.
[4] R.K. Gupta, R.W. Traill-Nash, Bridge dynamic loading due to road surface irregularities and braking of vehicle, *Earthquake Engineering and Structural Dynamics* 8 (1) (1980) 83–96.
[5] N.L. Mulcahy, Bridge response with tractor–trailer vehicle loading, *Earthquake Engineering and Structural Dynamics* 11 (5) (1983) 649–665.
[6] V.V. Krylov, Generation of ground vibrations by accelerating and braking road vehicles, *Acustica* 82 (4) (1996) 642–649.
[7] J. Toth, P. Ruge, Spectral assessment of mesh adaptations for the analysis of the dynamical longitudinal behavior of railway bridges, *Archive of Applied Mechanics* 71 (6–7) (2001) 453–462.
[8] Y.B. Yang, Y.S. Wu, A versatile element for analyzing vehicle–bridge interaction response, *Engineering Structures* 23 (5) (2001) 452–469.
[9] A. Berghuvud, Freight car curving performance in braked conditions, *Proceedings of The Institution of Mechanical Engineers Part F—Journal of Rail and Rapid Transit* 216 (1) (2002) 23–29.
[10] H.Y. Hu, Q. Han, Three dimensional modeling and dynamic analysis of four-wheel-steering vehicles, *Acta Mechanica Sinica* 19 (1) (2003) 79–88.
[11] R. Guner, N. Yavuz, O. Kopmaz, F. Ozturk, Validation of analytical model of vehicle brake system, *International Journal of Vehicle Design* 35 (4) (2004) 331–348.
[12] S.S. Law, X.Q. Zhu, Bridge dynamic responses due to road surface roughness and braking of vehicle, *Journal of Sound and Vibration* 282 (3–5) (2005) 805–830.
[13] L. Fryba, *Vibration of Solids and Structures under Moving Load*, Thomas Telford, London, 1999.
[14] S.H. Ju, K.S. Kung, Mass types, element orders and solving schemes for the Richards equation, *Computers and Geosciences* 23 (2) (1997) 175–187.
[15] S.H. Ju, Finite element analyses of wave propagations due to high-speed train across bridges, *International Journal for Numerical Method in Engineering* 54 (9) (2002) 1391–1408.
[16] S.H. Ju, 3D Finite element analyses of wave barriers for reduction of train-induced vibrations, *Journal of Geotechnical and Geoenvironmental Engineering—ASCE* 130 (7) (2004) 740–748.
[17] S.H. Ju, H.T. Lin, Analysis of train-induced vibrations and vibration reduction schemes above and below critical Rayleigh speeds by finite element method, *Soil Dynamics and Earthquake Engineering* 24 (12) (2004) 993–1002.